Dispersion of Refractoriness and Induction of Reentry due to Chaos Synchronization in a Model of Cardiac Tissue

Yuanfang Xie,[1] Gang Hu,[4] Daisuke Sato,[1] James N. Weiss,[1,2] Alan Garfinkel,[1,3] and Zhilin Qu[1,*]

[1]*Department of Medicine (Cardiology), David Geffen School of Medicine, University of California,*
Los Angeles, California 90095, USA
[2]*Department of Physiology, David Geffen School of Medicine, University of California, Los Angeles, California 90095, USA*
[3]*Department of Physiological Science, University of California, Los Angeles, California 90095, USA*
[4]*Department of Physics, Beijing Normal University, Beijing 100875, People's Republic of China*
(Received 19 January 2007; published 12 September 2007)

Ventricular fibrillation is a lethal condition caused by multiple chaotically wandering electrical wavelets in the heart, reentering their own and each other's territories. The development of effective therapies requires a detailed understanding of how these reentrant waves are initiated. In this Letter, we demonstrate a novel mechanism for inducing reentry, in which chaos synchronization causes large-scale heterogeneities of refractoriness transverse to the direction of propagation. These regions of increased refractoriness create localized conduction block, which induces spiral wave reentry.

In ventricular fibrillation, the cause of sudden cardiac death, multiple reentrant spiral wavelets meander across the heart muscle [1]. The development of fibrillation in cardiac tissue requires two key steps: the initiation of the first reentrant (spiral) wave and then the degeneration of this reentrant wave into multiple wavelets. Many previous studies have focused on how a single spiral wave degenerates into multiple wavelet fibrillation, through spiral wave breakup caused by dynamical instabilities or through fibrillatory conduction block due to regions of refractory tissue [2–5]. Clinically, however, it is extremely important to prevent the first step from occurring. Preventing the initiation of the first reentry is critical, since once reentry occurs, it is life threatening whether or not it decays to multiple wavelet fibrillation. The initiation of reentry requires two critical components: critically timed triggers (e.g., premature ventricular excitations) and critically heterogeneous tissue substrates [6,7]. The problem is then to understand how the triggers and the substrates are generated, and how they interact to cause reentry.

Spatial heterogeneities in refractoriness can be caused by a number of factors. They preexist in the normal heart, and are amplified in diseased hearts by remodeling. But heterogeneities can also be induced in purely homogeneous tissue, for example, by dynamical instabilities causing spatially discordant action potential duration (APD) alternans [8]. APD alternans is a beat-to-beat alternation in APD when a cardiac myocyte is paced periodically. Other more complex behaviors, such as chaos, can also occur at similar pacing rates, as has been shown both theoretically and experimentally [9–16]. These nonlinear behaviors have been shown to be caused either by action potential duration (APD) restitution properties [9,11,12,15], relating the present APD (and hence refractoriness) to the cell's preceding diastolic interval (DI), or by intracellular calcium cycling instabilities [11,17]. In the

presence of conduction velocity restitution, i.e., where wave front velocity is a function of the previous DI, cellular APD alternans can become discordant in space; i.e., APD alternates out of phase in neighboring regions, causing an APD gradient in space [8,18]. However, APD gradients due to conduction velocity restitution develop only in the direction of propagation, and so a symmetry breaking is still needed to get localized refractoriness to create the conduction block that induces reentry. In a recent study, Sato *et al.* [19] showed that this symmetry can be broken by a short-wavelength instability when alternans is driven by intracellular calcium cycling and the calcium-voltage coupling is negative, inducing APD gradients transverse to the direction of propagation. But this mechanism cannot induce large APD gradients, due to the strong diffusion of voltage.

In this Letter, we show a new dynamical instability, based on chaos synchronization, that induces large APD gradients in the direction transverse to propagation. Chaos synchronization was first studied by Pecora and Carroll [20] and subsequently by many authors (see Ref. [21] for review). In general, two or more identical chaotic systems can be synchronized by diffusive coupling. This synchronization occurs for certain coupling strengths, and at system sizes smaller than a critical value. In the synchronized mode, all the chaotic subsystems have identical trajectories, even though they started with different initial conditions. When synchronization of the chaotic elements is lost, which we refer to as chaos desynchronization, either spatiotemporal chaos or periodic solutions can result. In this study, we show that the loss of synchronization of cardiac cellular chaos results in macroscopic heterogeneities in refractoriness in the direction transverse to propagation, thereby facilitating localized conduction block to initiate reentry in cardiac tissue.

Chaos desynchronization in a homogeneous one-dimensional (1D) cable model.—The membrane voltage

of the 1D cable model is governed by the following partial differential equation [2,3,8], which is a continuous approximation to cardiac tissue:

$$\frac{\partial V}{\partial t} = -(I_{\text{ion}} + I_{\text{sti}})/C_m + D\frac{\partial^2 V}{\partial x^2}, \quad (1)$$

where V is the transmembrane potential, $D = 0.001 \text{ cm}^2/\text{ms}$ is the diffusion constant, and $C_m = 1 \text{ } \mu\text{F}/\text{cm}^2$ is the membrane capacitance. I_{sti} in Eq. (1) is the stimulation current density with intensity of $25 \text{ } \mu\text{A}/\text{cm}^2$ and duration of 2 ms, which was applied uniformly over the whole length of the cable. I_{ion} is generated under two conditions: (i) monotonic APD restitution [APDR1, Fig. 1(a)] with APD shortened by increasing the time-dependent potassium current by 50% and by changing the time constants of the gating kinetics of the slow inward current to 75% of their values in the original Beeler-Reuter model [22]; (ii) a modified Beeler-Reuter model [23] to give rise to a nonmonotonic APD restitution curve [APDR2, Fig. 1(b)]. The Beeler-Reuter model is an action potential model which has been widely used to investigate the action potential excitation and propagation dynamics in cardiac models [2,9,10,23]. Note that both types of APD restitution curves have been shown in experiments [12,15,18,24,25], and can give rise to alternans, chaos, and other complex dynamics during periodic stimulation [Figs. 1(c) and 1(d)], which has been shown in previous theoretical studies [9,10,23]. For APDR1, chaos occurs due to steep APD restitution and stimulation failure [Fig. 1(c)]. For APDR2, chaos occurs at slower pacing without stimulation failure [Fig. 1(d)]; i.e., each stimulus elicits an action potential.

Under uniform periodic pacing, the 1D cable model of Eq. (1) can become spatially desynchronized when the isolated cells are in the chaotic regime. In other words, although the cells are all identical and identically stimulated, their membrane potential can become very different over time. To quantitatively detect this desynchronization in simulating Eq. (1), we defined the standard deviation of the voltage as

$$\sigma = \lim_{T\to\infty}\frac{1}{T - T_0}\int_{T_0}^{T}dt\sqrt{\int_0^L[V(x,t) - \bar{V}(t)]^2 dx/L}, \quad (2)$$

where $\bar{V}(t)$ is average voltage over the whole cable at time t, T_0 is a time after the transient, and L is the length of the cable. Synchronization therefore occurs when σ approaches zero. A small (1% of the magnitude of each variable) random perturbation to the variables of Eq. (1) was given at time zero. If we pace a 6 cm cable with APDR1, σ approaches zero except in the chaotic regime [Fig. 2(a)], indicating that this instability only occurs when chaos is engaged. Note that desynchronization occurs only when L is greater than a critical length, a hallmark of chaos synchronization [Fig. 2(b)] [21]. Here we calculated the Lyapunov exponent λ versus the wave number k using the method of a previous study [26]. For a pacing cycle length (PCL) = 100 ms, λ becomes negative at $k_c \approx 3.6 \text{ cm}^{-1}$ [Fig. 2(c)]. Using the relation $L_c = \pi/k_c$ for no-flux boundary condition, one obtains $L_c = 0.87 \text{ cm}$, which agrees well with $L_c = 0.85$ obtained from the numerical simulation of the 1D cable [Fig. 2(b)]. The voltage distribution in space after desynchronization is illustrated in Figs. 2(d)–2(f), showing examples of space-time plots of voltage for APDR1 at PCL = 100 ms and for APDR2 at PCL = 310 ms and PCL = 160 ms, respectively. Although the initial perturbation is very small and random,
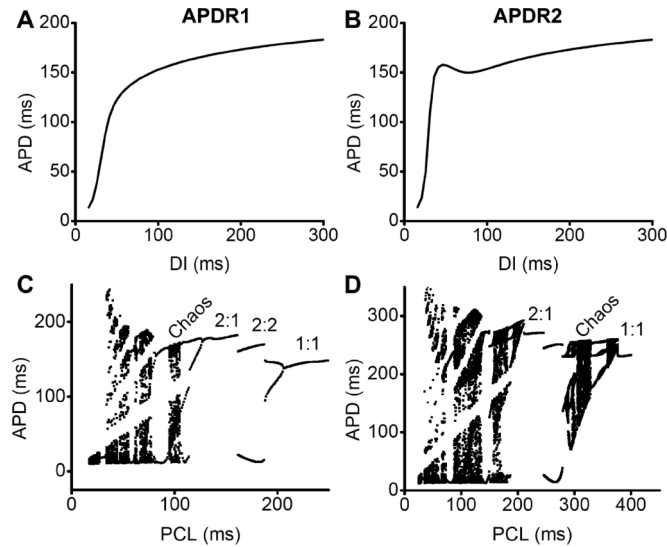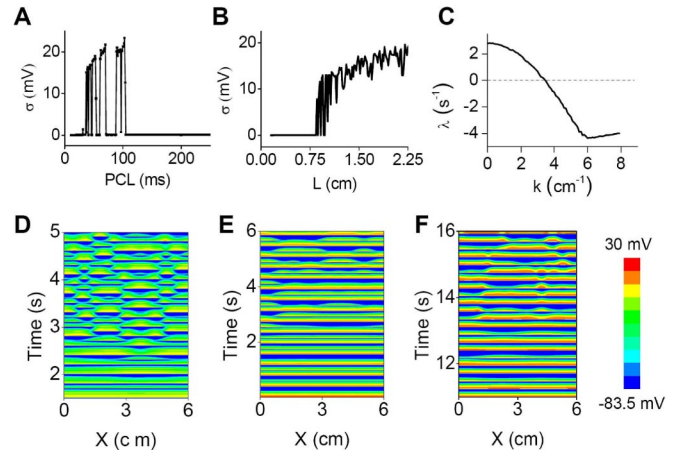

FIG. 1. (a) and (b) show APD restitution curves of the original Beeler-Reuter model with shortened APD and the modified Beeler-Reuter model, respectively; (c) and (d) show their corresponding bifurcation diagrams. Note the presence of stimulation failure in the passage to 2:1 conduction in (c) and (d).

FIG. 2 (color online). (a) σ versus PCL in a 6 cm cable with APDR1; (b) σ versus cable length L for PCL = 100 ms [in the chaotic regime of (d)]; (c) Lyapunov exponent λ versus wave number k for PCL = 100. (d)–(f) Space-time plots of voltage for APDR1 with PCL = 100 ms, APDR2 with PCL = 310 ms and PCL = 160 ms, respectively. To break the initial symmetry, a small random perturbation (1% of the magnitude of each variable) was given at time zero, and for all other simulations in the present study.

the resulting heterogeneities are substantial, and importantly, are organized over macroscopic spatial scales.

Induction of dispersion of refractoriness and spiral wave reentry in a homogeneous two-dimensional (2D) tissue model.—The diffusion of voltage in a 2D tissue model is described by the following differential equation [2–4]:

$$\frac{\partial V}{\partial t} = -(I_{\text{ion}} + I_{\text{sti}})/C_m + D\left(\frac{\partial^2 V}{\partial x^2} + \frac{\partial^2 V}{\partial y^2}\right), \quad (3)$$

where the parameters are the same as for Eq. (1). I_{sti} was applied only in a region of the tissue, instead of the whole tissue as used in the 1D cable.

In this first case, I_{sti} was applied in a narrow strip (0.3×7.5 cm^2) spanning the left border of the tissue, inducing planar waves propagating from left to right. For APDR1 at PCL = 100 ms, chaos desynchronization was first induced in the region around the pacing site, followed by local conduction block and eventually complex reentrant patterns [Figs. 3(a) and 3(b); [27] movie 1]. In fact, for the original Beeler-Reuter model without the APD shortening, the bifurcation is similar to the case shown in Fig. 1(c) and chaos desynchronization also occurs in the 1D cable. However, in this case, reentry could not be induced by pacing a narrow strip, but could be induced by pacing a larger area (see [27], movies 2 and 3). For APDR2, chaos desynchronization was observed at PCL = 310 ms, resulting in very heterogeneous refractoriness, although no conduction block or reentrant wave fronts were formed [Figs. 3(c) and 3(d); [27] movie 4]. In this case, chaos occurred without the requirement of stimulation failure and thus each wave could successfully propagate through the whole tissue without blocking. Indeed, when paced faster, at PCL = 160 ms, chaos desynchronization did lead to localized conduction block and reentry [Figs. 3(e) and 3(f); [27] movie 5] since chaos occurred after the 2:1 block [Fig. 1(d)]. Since chaos desynchronization and stimulation

failure occur in the pacing area, the spiral wave tends to first form close to the pacing area as shown in Figs. 3(a) and 3(e).

In a second experiment, I_{sti} was applied in a 0.15×0.15 cm^2 area at the lower-left corner of the tissue, inducing concentric "target" waves. For APDR1 at PCL = 100 ms, activation was chaotic, but no transverse instability occurred to induce localized dispersion of refractoriness, so reentry was not initiated [Fig. 4(a)]. But for APDR2 at PCL = 310 ms, a transverse instability occurred, initially symmetric with respect to the diagonal line (since boundary effects are also symmetric with respect to the diagonal line), but the symmetry was eventually broken [Fig. 4(b); [27] movie 7]. If we delivered a single stimulus at a shorter interval to the same location, reentry could be induced [Fig. 4(c); [27] movie 8]. The reason that transverse instability does not occur with APDR1, but can occur with APDR2, is as follows. In the monotonic case, although chaos occurred at the pacing site, there were many attenuated or small amplitude action potential activations that could not successfully propagate out of the pacing area, resulting in a slower activation rate in tissue distant from the pacing site [Fig. 4(d)]. The average cycle length at the pacing site was 100 ms, but was 218 ms elsewhere. Note that at PCL = 218 ms, the isolated cell is in a stable steady state regime [Fig. 1(c)]. Although the activation inside the tissue is nonperiodic [Fig. 4(d)], it is not dynamical chaos. Instead, it just represents passive responses to the irregular activation averaging 218 ms emanating from the pacing site. Therefore, the wave front propagation out of the pacing area is intrinsically stable and no chaos desynchronization can occur. However, in the nonmonotonic case, every
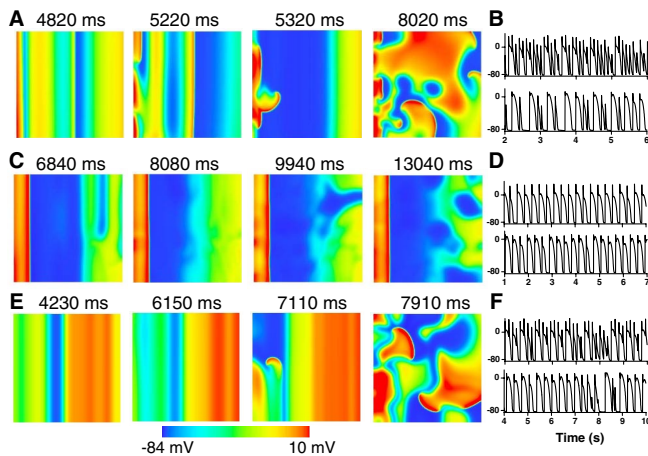

FIG. 3 (color online). Shown are voltage snapshots and voltage traces for APDR1 with PCL = 100 ms [(a),(b)]; APDR2 with PCL = 310 ms [(c),(d)], and PCL = 160 ms [(e),(f)]. The voltage traces were recorded from the pacing strip (upper panels) and the tissue center (lower panels).
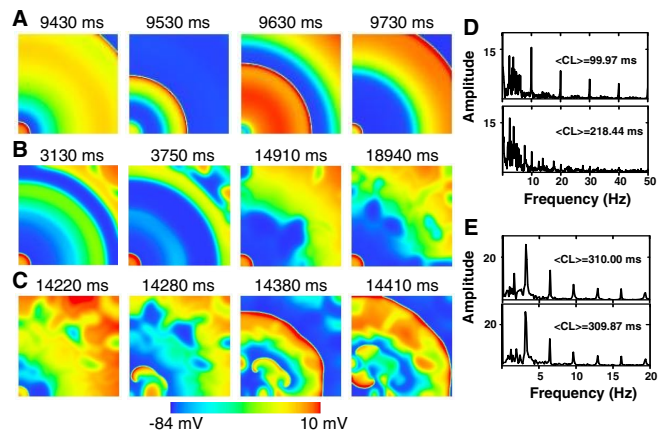

FIG. 4 (color online). (a) Voltage snapshots for APDR1 with PCL = 100 ms. (b) Voltage snapshots for APDR2 with PCL = 310 ms. (c) Reentry was induced by a premature stimulation at the same location with a coupling interval 260 ms, following the induced heterogeneity in (b). (d),(e) FFT spectra of voltage from the pacing site (upper panel) and from the tissue center (lower panel) for (a) and (b), respectively. The averaged cycle length ⟨CL⟩ was indicated for each panel.

excitation can successfully propagate through the whole tissue, and thus the activation rates are the same everywhere [Fig. 4(e)]; i.e., every cell is activated by the same average cycle length of 310 ms. At this rate, each cell is in its intrinsically chaotic regime [see Fig. 1(d)], so that chaos desynchronization occurs once the length of the wave front exceeds the critical length.

Conclusions and discussion.—Previous studies [2–4] on chaotic dynamics in cardiac tissue focused on how spiral breakup leads to spatiotemporal chaos. Here, by contrast, we study a quite different situation, and show how chaotic individual cardiac cells (under rapid periodic stimulation) can synchronize and desynchronize in tissue to cause transverse instabilities resulting in localized regions of increased refractoriness. This represents a novel mechanism for reentry induction in cardiac tissue. We simulated two pacing protocols—simultaneous stimulation of either a narrow strip in the tissue or a small 2D region. In real cardiac systems, the first protocol corresponds most closely to stimulation from a supraventricular tachycardia (originating from the sinus node or otherwise) engaging the His-Purkinje conduction system, which can nearly simultaneously activate the endocardium of the ventricles. The second protocol corresponds to an automatic or triggered beat arising from a focus in the ventricles or atria. One interesting observation is that when APD restitution is monotonic, transverse instabilities can only be induced by stimulation of a strip, but not by point stimulation. In contrast, both protocols can induce transverse instabilities when APD restitution is nonmonotonic. Nonmonotonic APD restitution has been observed in cardiac systems [15,24,25], and the present study illuminates its importance in cardiac arrhythmogenesis. Our findings may apply primarily to rapid heart rhythms which induce chaotic behavior [9,10,13–15], which could potentially cause them to degenerate into fibrillation by this chaos synchronization or desynchronization mechanism. However, dynamical instabilities, such as pulsus alternans and *T*-wave alternans, can occur at near normal heart rates in diseased hearts [28,29], so that chaos might also occur at near normal heart rates in this setting. Nevertheless, fast heart rates do occur in the heart, such as sinus tachycardia or ventricular tachycardia due to periodic focal excitations. Although a real heart is always heterogeneous, we expect that chaos desynchronization will interact with the preexisting heterogeneities to synergistically promote the critical refractory gradient required for initiation of reentry.

*zqu@mednet.ucla.edu

[1] D. P. Zipes and H. J. Wellens, Circulation **98**, 2334 (1998).
[2] M. Courtemanche, Chaos **6**, 579 (1996).
[3] A. Karma, Chaos **4**, 461 (1994).
[4] Z. Qu *et al.*, Ann. Biomed. Eng. **28**, 755 (2000).
[5] A. V. Zaitsev *et al.*, Circ. Res. **86**, 408 (2000).
[6] A. T. Winfree, J. Theor. Biol. **138**, 353 (1989).
[7] K. R. Laurita and D. S. Rosenbaum, Circ. Res. **87**, 922 (2000).
[8] Z. Qu *et al.*, Circulation **102**, 1664 (2000).
[9] T. J. Lewis and M. R. Guevara, J. Theor. Biol. **146**, 407 (1990).
[10] A. Vinet *et al.*, Circ. Res. **67**, 1510 (1990).
[11] Z. Qu, Y. Shiferaw, and J. N. Weiss, Phys. Rev. E **75**, 011927 (2007).
[12] J. B. Nolasco and R. W. Dahlen, J. Appl. Physiol. **25**, 191 (1968).
[13] M. R. Guevara, L. Glass, and A. Shrier, Science **214**, 1350 (1981).
[14] D. R. Chialvo, R. F. Gilmour, and J. Jalife, Nature (London) **343**, 653 (1990).
[15] M. Watanabe, N. F. Otani, and R. F. Gilmour, Circ. Res. **76**, 915 (1995).
[16] N. F. Otani and R. F. Gilmour, J. Theor. Biol. **187**, 409 (1997).
[17] Y. Shiferaw *et al.*, Biophys. J. **85**, 3666 (2003).
[18] J. M. Pastore *et al.*, Circulation **99**, 1385 (1999).
[19] D. Sato *et al.*, Circ. Res. **99**, 520 (2006).
[20] L. M. Pecora and T. L. Carroll, Phys. Rev. Lett. **64**, 821 (1990).
[21] L. M. Pecora *et al.*, Chaos **7**, 520 (1997).
[22] G. W. Beeler and H. Reuter, J. Physiol. **268**, 177 (1977).
[23] Z. Qu, J. N. Weiss, and A. Garfinkel, Phys. Rev. Lett. **78**, 1387 (1997).
[24] M. R. Franz *et al.*, Circ. Res. **53**, 815 (1983).
[25] J. M. Morgan, D. Cunningham, and E. Rowland, J. Am. Coll. Cardiol. **19**, 1244 (1992).
[26] Z. Qu, F. Xie, and A. Garfinkel, Phys. Rev. Lett. **83**, 2668 (1999).
[27] See EPAPS Document No. E-PRLTAO-99-056736. For more information on EPAPS, see http://www.aip.org/pubservs/epaps.html.
[28] D. S. Rosenbaum *et al.*, N. Engl. J. Med. **330**, 235 (1994).
[29] B. Suys, R. De Paep, and K. Francois, Circulation **108**, e36 (2003).